Title: Oscillations support co-firing of neurons in the service of human memory formation

Authors: Frédéric Roux[1], George Parish[1], Ramesh Chelvarajah[1,2], David T. Rollings[2], Vijay Sawlani[1,2,] Hajo Hamer[3], Stephanie Gollwitzer[3], Gernot Kreiselmeyer[3], Marije Ter Wal[1], Luca Kolibius[4], Bernhard Staresina[1], Maria Wimber[4], Matthew W. Self[5], Simon Hanslmayr*[4]

Affiliations:

[1]School of Psychology, University of Birmingham, Birmingham B15 2TT, United Kingdom

[2]Complex Epilepsy and Surgery Service, Neuroscience Department, Queen Elizabeth Hospital, Birmingham B15 2TH, United Kingdom

[3]Epilepsy Center, Department of Neurology, University Hospital Erlangen, 91054 Erlangen, Germany

[4]Institute of Neuroscience and Psychology, University of Glasgow, Glasgow G12 8QB, United Kingdom

[5]Department of Vision and Cognition, Netherlands Institute of Neuroscience, an institute of the Royal Netherlands Academy of Art and Sciences (KNAW), Amsterdam, the Netherlands

Abstract: Brain oscillations have been demonstrated to support information transfer between neurons in animal models of memory. However, direct evidence for a similar role of oscillations in humans has so far remained unclear. Here we show that theta and gamma oscillations in the medial-temporal-lobe synchronize neural firing during a memory task. We observe that faster oscillations at theta- and gamma frequencies correlate with co-firing of neurons at short latencies (~20-30 ms) and occur during successful memory formation. Slower oscillations in these same frequency bands, by contrast, correlate with longer co-firing latencies and occur during memory failure. A computational model supports the present effects and links these findings to synaptic plasticity. Together, the results support the long-standing assumption that correlated neural firing supports human episodic memory formation.

One Sentence Summary: Theta and gamma oscillations induce co-firing of neurons in the human medial temporal lobe during successful memory formation.

Main Text: Episodic memory relies on synaptic modifications transforming fleeting experiences into durable memory traces (*1*). The strengthening of synaptic connections between neurons that are active during the experience of an episode in turn critically depends on the temporal structure of neural firing (*2-5*). Evidence that has accumulated over several decades suggests that coordinated rhythmic activity may provide a candidate mechanism to impose a fine-grained temporal structure on neural firing (*6-9*). Accordingly, brain oscillations at theta (~3 – 9 Hz) and gamma (~ 40 – 80 Hz) frequencies in the human medial temporal lobe (MTL), a brain structure critical for memory (*10*), have been proposed to promote the formation of memories through the synchronization of neural firing in the MTL (*11, 12*).

While it has long been assumed that correlated neural firing is fundamentally involved in the strengthening of synaptic connections (*4*) the mechanisms of memory formation in the human brain have remained largely unknown. Evidence suggests that synchronization of neurons to theta oscillations (*13*), as well as the presence of fast gamma oscillations (*14*) represent favorable conditions for human memory formation. However, so far, the role of theta and gamma oscillations in mediating synchronous neural firing in humans during memory formation has remained unclear. This study fills this gap by providing novel evidence of synchronous neural firing coupled to the frequency of theta and gamma rhythms recorded from micro-wire electrodes during an associative episodic memory task (Figure 1A). The mechanistic implications of the present findings for synaptic plasticity are supported by a computational model that highlights a functional role of neural oscillations in modulating the strength of spike-timing-dependent-plasticity (STDP)(*3*).

Memory task and behavior

Nine patients with refractory epilepsy participated in 44 sessions of an associative episodic memory task (Figure 1A). During the encoding phase of the task, the patient was presented with several trials each containing a picture of an animal (cue), which was shown for 2 seconds. Then a pair of images appeared which either showed a face and a place, two faces or two places. The patients were instructed to link the three elements of the episode together by mentally imagining a narrative (e.g. "*I saw a tiger in the zoo with Stephen Fry*") and press a button to indicate whether the invented narrative or combination of images was plausible or implausible, then the next trial followed. After the encoding phase and a brief distractor test, memory performance was assessed by means of a cued recall test. During the test phase the picture of the animal was presented for 2 seconds and the patient indicated how many stimuli they could remember (0, 1 or 2). Then a screen with four images appeared, and the patient selected the two images that they thought were paired with the cue originally. Trials for which both images were correctly recalled are labelled 'hit', all other trials (i.e. 1 image or both wrong) are labelled 'miss'. Therefore, contrasting hits with misses isolates neural processes which support the complete memorization of an episode (as opposed to incomplete memories or no memory at all). Any such process has to start when the full memory information is present, which is at the onset of the face/place images (i.e. 2 seconds). Therefore, all subsequent analysis focused on this time window (2-3 seconds; highlighted in Figure 1A).

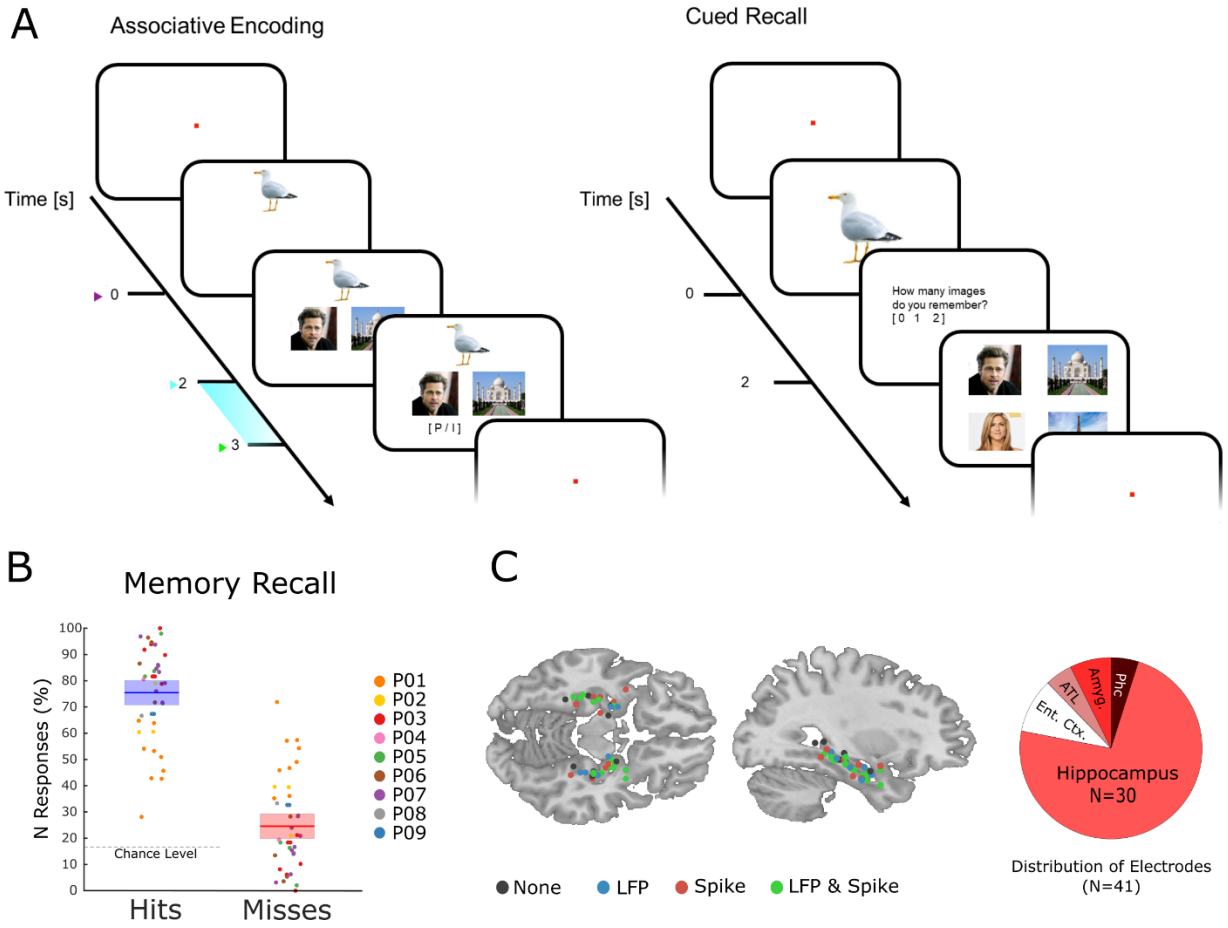

Figure 1. The memory task and behavioral results. (A) During encoding patients had to memorize triplets of stimuli consisting of an animal, and a face and a place (or two faces, or two places). The light blue bar highlights the time that was used for analysis. (B) Memory performance during the cued recall test is shown for all patients and sessions. Note that chance level is 16.6%. (C) Electrode locations are plotted overlaid onto a template brain in MNI space. Color codes indicate whether an electrode provided LFP, Spiking, both, or no data. The pie chart on the right shows the distribution of electrodes across MTL regions (Ent. Ctx.: Entorhinal Cortex; ATL.: Anterior Temporal Lobe; Amyg.: Amygdala; Phc.: Parahippocampal Cortex).

On average patients correctly recalled both associated items on 75.43% (s.d.: 13.3) of the trials (Figure 1B). Note that this is well above chance level (16.6%). The remaining miss trials were approximately evenly distributed between incomplete memories (i.e. only one association recalled; 12.6%) or completely forgotten (i.e. both incorrect; 11.9%).

Fast gamma oscillations synchronize neurons locally and correlate with successful memory

Neural spiking and LFP activity were recorded with Behnke-Fried hybrid depth-electrodes from MTL regions (Figure 1C). The majority of electrodes (73%) were located in the hippocampus, the rest was located in adjacent MTL regions. Altogether 232 putative single and multi-units were recorded, of which 218 were used for further analysis (14 units were rejected because of too low firing rates; see Supplementary Methods). Neural firing during encoding was not modulated by memory for the time window of interest (2-3 seconds). However, hits showed a sustained increase in firing rate compared to misses at a later time window (>3 seconds; Figure S1). LFPs for hits and

misses also did not differ in terms of event-related potentials or inter-trial phase coherence (Fig. S2, S3C-D), but showed expected differences in broad band power(*15*), with hits showing decreased low frequency but increased high frequency power (Fig. S3A-B).

Synchronization of neural firing of an individual neuron to the population activity can be measured with spike-field coupling (SFC). SFC can occur at two different spatial levels, locally (within a region) or distally (across regions; see Methods; Figure 2A). Locally, SFC indicates the firing of a neuron being entrained to its surrounding LFP. Distally, SFC indicates that the firing of one neuron elicits post-synaptic currents in another region and is therefore interpreted as a functional measure of connectivity; the spike providing region is the up-stream sender, and the LFP providing region the down-stream receiver(*16-18*). Accordingly, we split spike-LFP pairs into these two categories, i.e. local and distal couplings. SFC was measured with the pairwise phase-consistency index (PPC)(*19*), which was preferred over other measures because it is not biased by the number of observations (e.g., spikes, trials).

During the time window of interest (2-3 seconds), 192 significantly (Rayleigh test; $p_{corr}<0.05$; FDR-correction) coupled spike-LFP pairs were found in the high-frequency range (40-80 Hz), of which 53 were coupled to the local LFP and 139 coupled to distal LFPs (Figure 2A). The number of locally coupled pairs was significantly higher than chance (Randomization test; $p<0.0001$), whereas the number of distally coupled pairs was not ($p>0.5$). Local spike-field coupling showed a pronounced peak in the fast gamma range (~65 Hz), which was substantially stronger compared to distal couplings (T-test; $p_{corr}<0.05$; Figure 2B; FDR-correction). Importantly, the peak frequency of local spike-field coupling varied as a function of memory formation such that hits showed stronger spike-field coupling at a higher frequency (~70 Hz) than misses (~62Hz; T-test; $p_{corr}<0.05$; FDR-correction; Figure 2C). This effect was also significant when using sessions as random variable (T-test; $t_{19}=2.21$; $p<0.05$).

This pattern suggests a shift in frequency, with hits showing spike-field coupling at a higher gamma frequency compared to misses. This intuition was confirmed by a peak detection analysis where gamma peak frequencies for hits and misses for each spike-field pair were extracted and compared (T-test; $t_{36}=1.96$; $p<0.05$; Figure 3D). Figure 3E shows this effect for one example unit, which couples to a slightly slower gamma rhythm for misses compared to hits. A control analysis, which effectively controls for a possible selection bias due to unbalanced trial numbers revealed similar results (Figure S4B).

Taken together, fast gamma oscillations temporally organize spikes within a region. Later fully remembered episodes (hits) are distinguished from incomplete or forgotten episodes (misses) by the frequency to which spikes are coupled to; with fast gamma oscillations benefiting memory formation, and slow gamma oscillations being detrimental for memory formation. This effect is unlikely to be caused by differences in stimulus evoked activity since neither ERPs nor firing rate showed a memory related difference in the time window of interest (Fig. S2-S3). These differences are also unlikely to be caused by differences in signal-to-noise ratio in the LFP, which can potentially affect measures of phase consistency(*20*), because power did not show a similar shift in frequency as observed for spike-field coupling, but rather replicated previously described broad band effects (Fig S3A-B).

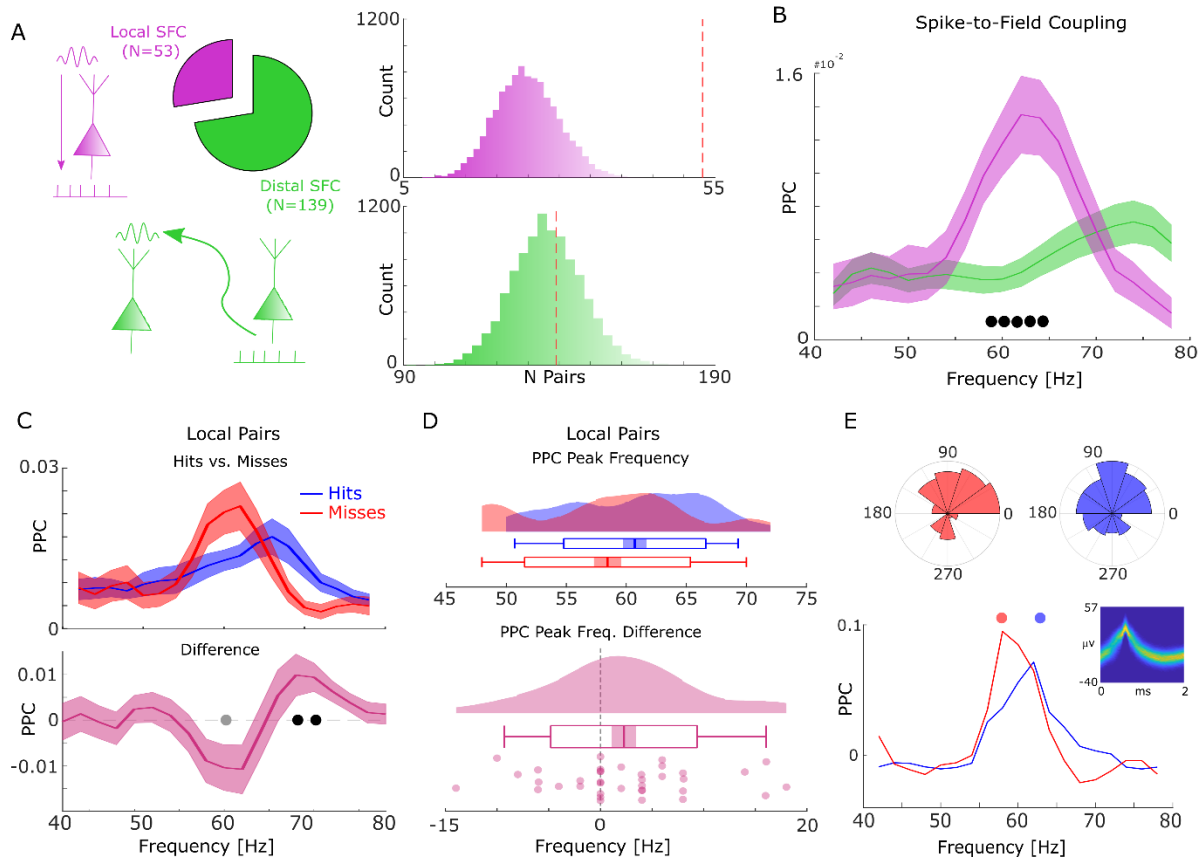

Figure 2. Spike-field coupling results for gamma. (A) Number of significant (p_{corr}<0.05) locally (pink) and distally (green) coupled spike-field pairs are shown. The histograms on the right show the results of a randomization procedure testing how many pairs would be expected under the null hypothesis (see Methods). (B) Pairwise phase consistency (PPC) is plotted for local and distal spike-field pairs. Filled circles indicate significant differences (p_{corr}<0.05). Shaded areas indicate standard error of the mean. (C) Pairwise phase consistency (PPC) is shown separately for hits and misses (top panel), and for the difference between the two conditions (bottom panel) for locally coupled spike-field pairs. Filled black circles indicate significant differences (p_{corr}<0.05). Grey circles indicate statistical trends (p_{uncorr}<0.05). Shaded areas indicate standard error of the mean. (D) Peak frequency in PPC across all spike-field pairs is shown for hits and misses (top), and for the difference (hits-misses, bottom). The solid bar indicates the mean, shaded areas indicate standard error, the box indicates standard deviation, and the bars indicate 5th and 95th percentiles. (E) Local gamma spike-field coupling is shown for one example putative multi-unit recorded from the entorhinal cortex. Phase histograms on top indicate phase distribution for hits at 62 Hz (blue) and misses at 58 Hz (red). Spike wave shapes on the right are plotted by means of a 2D histogram.

Fast theta oscillations synchronize neurons distally and correlate with successful memory

The same spike-field coupling analysis as above was carried out for the low frequency ranges (2 – 40 Hz). We identified 103 locally coupled, and 387 distally coupled spike-field pairs (Rayleigh-test; p_{corr}<0.05; FDR corrected; Figure 3A). For both local and distal couplings the number of significant pairs exceeded chance level (Randomization test; both p<0.0001). Local couplings showed a peak PPC at around 5 Hz (and another peak at 13 Hz), whereas distal couplings showed a peak at around 8-9 Hz. Local spike-field couplings were robustly stronger than distally coupled pairs in the beta frequency range (20-30 Hz).

Distal, but not local spike-field coupling varied as a function of memory success. Distally coupled spike-field pairs showed stronger coupling for hits compared to misses in the fast theta frequency range (8-10 Hz) and higher spike-field coupling for misses compared to hits in the lower theta frequency range (5 Hz; Figure 4B, T-test; $p<0.05$; FDR-corrected). The stronger spike-field coupling in the fast theta band for hits compared to misses was also found to be significant when using sessions (T-test; $t_{20}=3.25$; $p<0.005$) as random variable. No significant differences between hits and misses were obtained for locally coupled spike-field pairs.

Like the memory related difference in gamma peak frequency, a shift in peak frequency also drove the memory-related difference in distal theta spike-field coupling. This was confirmed by a peak detection analysis showing that hits exhibited a slightly faster peak in theta spike-field coupling compared to misses (T-test; $t_{206}=3.49$; $p<0.0001$; Figure 3D). This effect is shown for one example unit which is distally coupled to a slow theta oscillation for misses, and to a fast theta oscillation for hits (see Figure S4A for control analysis on selection bias). Like the effects in local gamma coupling these effects are unlikely to be due to changes in stimulus evoked activity (Fig. S2-S3).

In agreement with the results obtained for local gamma oscillations we observed that distal theta spike-LFP coupling varied as a function of memory formation, with hits showing coupling at faster theta peak frequencies compared to misses. Thus, the present findings reveal two distinct cell populations that synchronize either to local gamma rhythms or distal theta rhythms, and a functional relationship between the peak frequency of gamma and theta rhythms and memory formation.

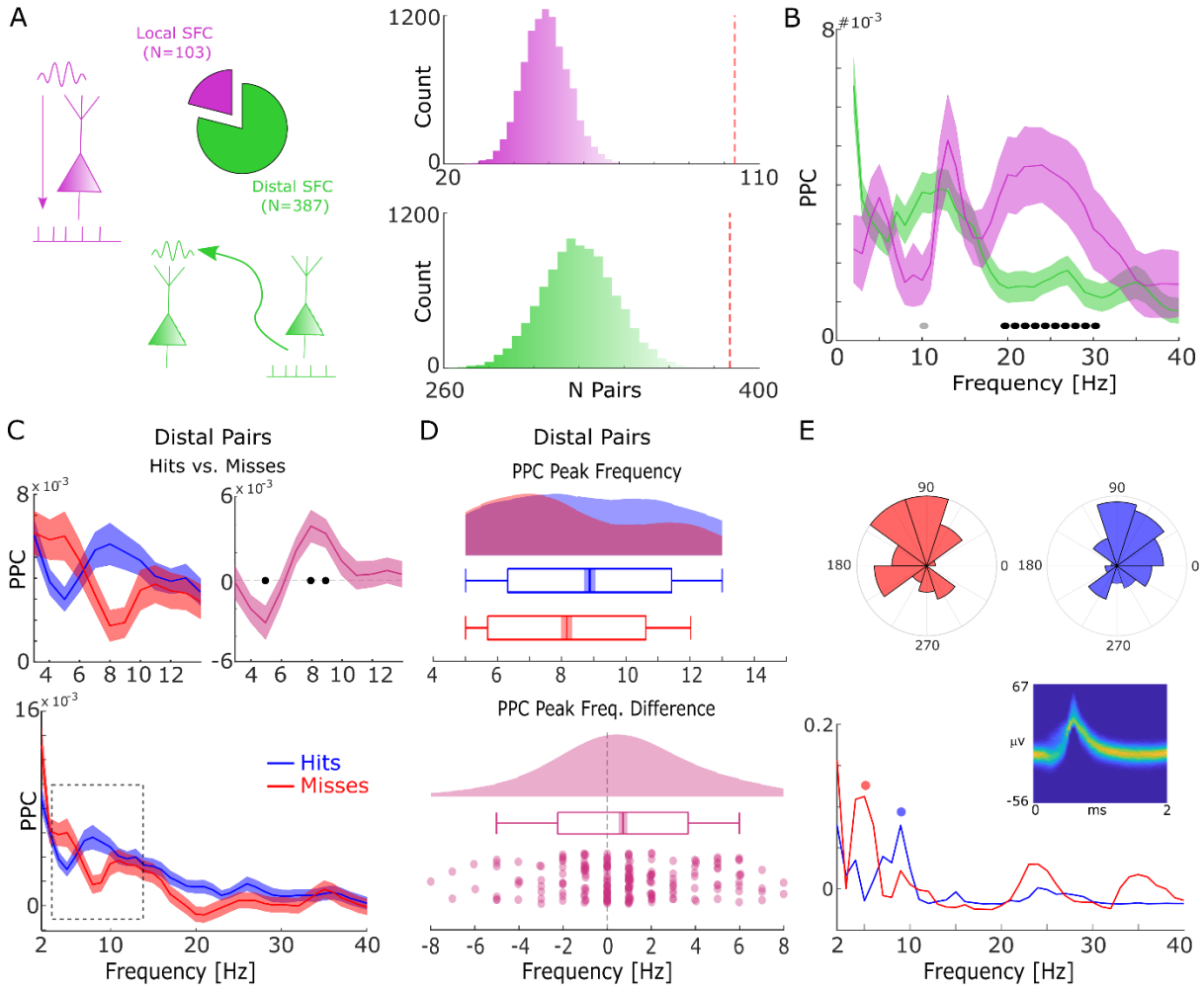

Figure 3. Spike-field coupling results for the lower frequencies. (A) Number of significant (p_{corr}<0.05) locally (pink) and distally (green) coupled spike-field pairs are shown. The histograms on the right show the results of a randomization procedure testing, with the red dashed line indicating the empirically observed value. (B) PPC is plotted for local and distal spike-field pairs. Filled circles indicate significant differences (p_{corr}<0.05). Grey circles indicate trends (p_{uncorr}<0.05). Shaded areas indicate standard error of the mean. (C) PPC is shown separately for hits (blue) and misses (red), and for the difference between the two conditions (magenta) for distally coupled spike-field pairs. The top panels show PPC values for the theta frequency range, the bottom panel shows all frequencies up to 40 Hz. Shaded areas indicate standard error of the mean. Filled circles indicate significant differences (p_{corr}<0.05). (D) Peak frequency in PPC across all distal spike-field pairs is shown for hits and misses (top), and for the difference (hits-misses). Box plots indicate the same indices as in Fig 2D. (E) Distal theta spike-field coupling is shown for one example unit recorded from the left posterior hippocampus, and the LFP recorded from the left entorhinal cortex. Phase histograms on top indicate phase distribution for hits at 9 Hz (blue) and misses at 5 Hz (red). Spike wave shapes on the right are plotted by means of a 2D histogram.

Theta and gamma oscillations are coupled for hits but not for misses

The above results show that successful memory formation relies on gamma oscillations synchronizing neurons at a local level, and theta oscillations at ~8 Hz synchronizing neurons across regions. Intriguingly, peak frequencies of both oscillations showed a similar relationship with memory formation, with faster frequencies being associated with successful memory. This raises

the question of whether gamma and theta oscillations are also temporally coordinated. For this analysis we considered electrodes from regions where the LFP was locally coupled to spikes in the gamma range and distally coupled to spikes in the low frequency (theta) range. More than half of the electrodes (58%) were available for this analysis (Figure 4A). Cross-frequency coupling was calculated by means of phase-amplitude coupling using the modulation index(*21*). Importantly, theta and gamma frequencies were adjusted to their peak frequency for each condition to account for the systematic difference in peak frequencies between hits and misses and to ensure the presence of a physiologically meaningful oscillation in both conditions(*22*). Theta phase to gamma power coupling was evident in single trials (Figure 4B-C). Hits showed stronger theta phase to gamma amplitude coupling compared to misses (Figure 4D; Wilcoxon test; $z=3.7$; $p<0.00001$). This increased cross-frequency coupling for hits compared to misses was also significant when pooling the data across sessions (Wilcoxon test; $p<0.05$). Cross-frequency coupling can be subject to several confounds, which we addressed by a series of control analyses (Supplementary Material and Fig. S5).

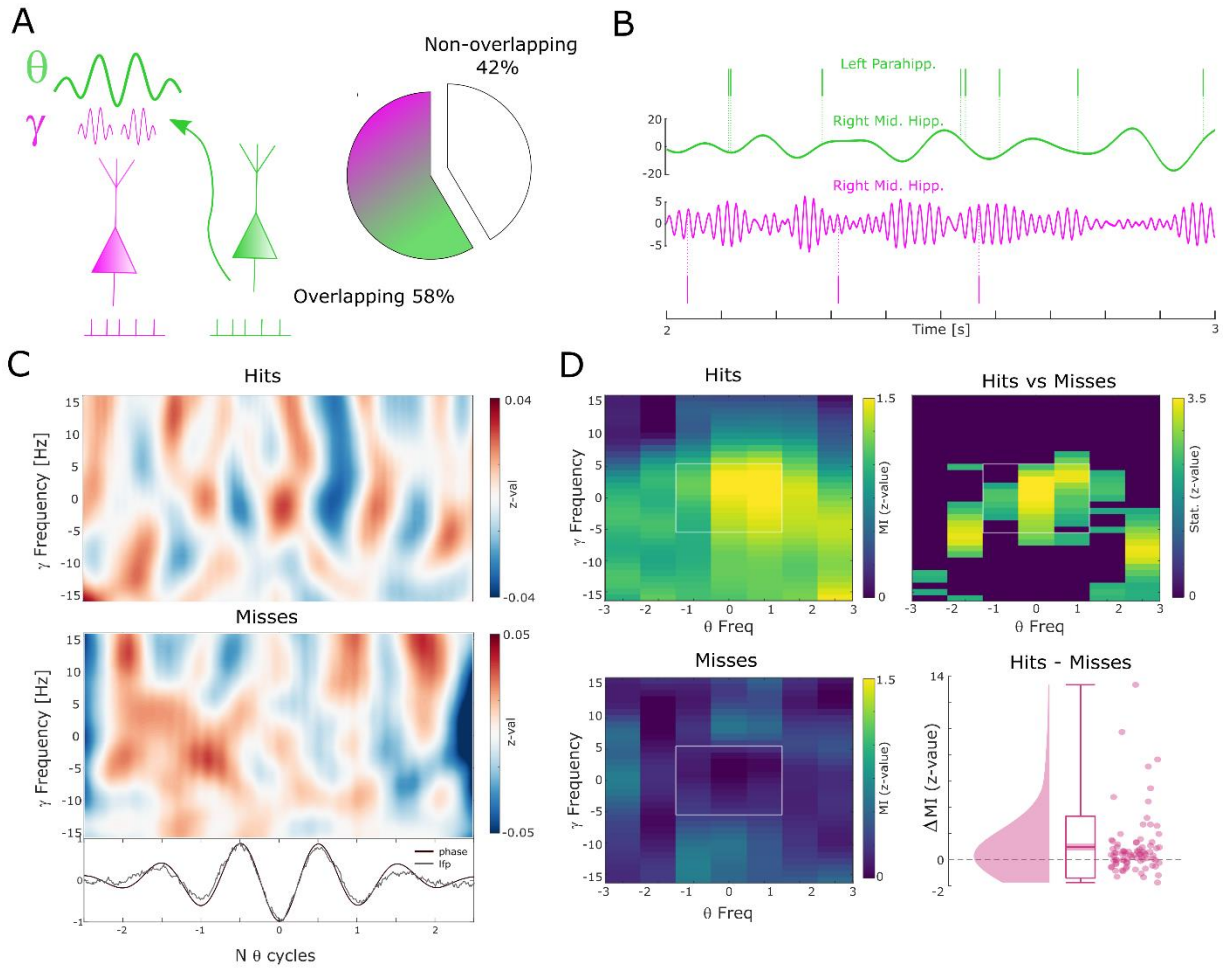

Figure 4. Theta to gamma cross frequency coupling results. (A) Percentage of overlapping local gamma (pink) and distal theta (green) spike-field pairs are shown. (B) Spikes and band-pass filtered LFP data for one example single trial are shown. The top row shows spikes from a unit in the left parahippocampal cortex which are coupled to the LFP in the right middle hippocampus (green). The gamma LFP from the same region (right mid hippocampus) is shown below (pink) as well as spikes from a unit in the same region that is coupled to this gamma oscillation. Note

the gamma power increase around theta troughs. (C) Theta phase sorted gamma power (y-axis centered to gamma peak frequency) is shown for all trials for the data shown in (C). The bottom panel shows averaged normalized band-pass filtered LFP data (black) and unfiltered LFP data (grey). (D) Co-modulograms are shown for hits and misses. Modulations indices (*21*), which indicate the strength of cross-frequency coupling, are plotted in terms of z-values where means and standard deviations were obtained from a trial shuffling procedure. The difference between hits and misses is shown as z-values obtained from a non-parametric Wilcoxon signrank test masked with $p_{corr}<0.05$ (FDR-corrected). The panel in the bottom right shows the individual differences between hits and misses across the whole dataset (N=83 pairs).

Short co-firing latencies predict successful memory formation

Brain oscillations have been proposed to establish efficient communication between neural ensembles*(6)*, with faster frequencies reflecting tighter synchronization of spikes. The effect on a downstream neuron of such a tighter synchronization upstream is that it is more likely to fire at all, and more likely to fire at an earlier time point*(7)*. Therefore, the faster theta and gamma oscillations observed for hits may reflect more efficient information transmission between theta-gamma coupled neural pairs. In order to test this hypothesis, we analyzed co-firing of neurons at different time lags by computing the cross-correlation of spike trains between putative theta up-stream units (i.e. the distally coupled unit) and their corresponding putative gamma down-stream unit (i.e. the locally coupled unit; Figure 5A). Overall, 32 pairs were available for this analysis, 24 of which showed above threshold co-firing (Supplementary Methods). Cross-correlations for hits and misses were each compared to a trial-shuffled baseline and transformed to z-scores effectively eliminating biases introduced by different trial numbers.

Compared to baseline, hits showed significant above chance co-firing at lags 20-40ms, whereas co-incidences for misses peaked at 60 ms (T-test; $p_{corr}<0.05$; FDR-correction; Figure 5B). In addition, hits showed stronger co-firing compared to misses at 20 ms (T-test; $p_{corr}<0.05$; FDR-correction; Figure 5B). A peak detection analysis revealed that co-firing for hits peaked significantly earlier compared to misses ($t_{21}=-3.2$; $p<0.005$; Figure 5B). This result held also when using a more conservative approach, i.e., pooling the data across number of neurons ($t_{11}=-3.34$; $p<0.01$). Intriguingly, this memory related co-firing effect was observed only when selecting pairs of neurons that were both locally coupled to gamma, and distally coupled to theta. Analyzing all possible pairs of distally coupled theta units showed no differences in peak co-incidences between hits and misses ($t_{126}=-0.78$; $p>0.4$). This is quite remarkable given that statistical power for this latter analysis was substantially higher. This pattern of results suggests that the coupling of down-stream neurons to local fast gamma oscillations is crucial for observing the memory dependent effect of co-firing at critical time windows. In order to test for a similar effect in the reverse direction (i.e. local gamma coupled neuron --> distal theta coupled neuron) the same co-incidence analysis was carried out for negative lags. Intriguingly, and consistent with the STDP framework, whereby a negative time lag leads to a decrease of synaptic connectivity*(2-3)*, misses showed peak co-firings at shorter negative latencies (i.e. closer to 0) compared to hits (Fig. S6; $t_{20}=-2.82$; $p<0.05$).

Together, these results suggest that successful memory formation correlates with shorter latencies of co-firing between putative down-stream and putative up-stream neurons. Notably, this effect is selective for neuron pairs that are both distally theta coupled and locally gamma coupled.

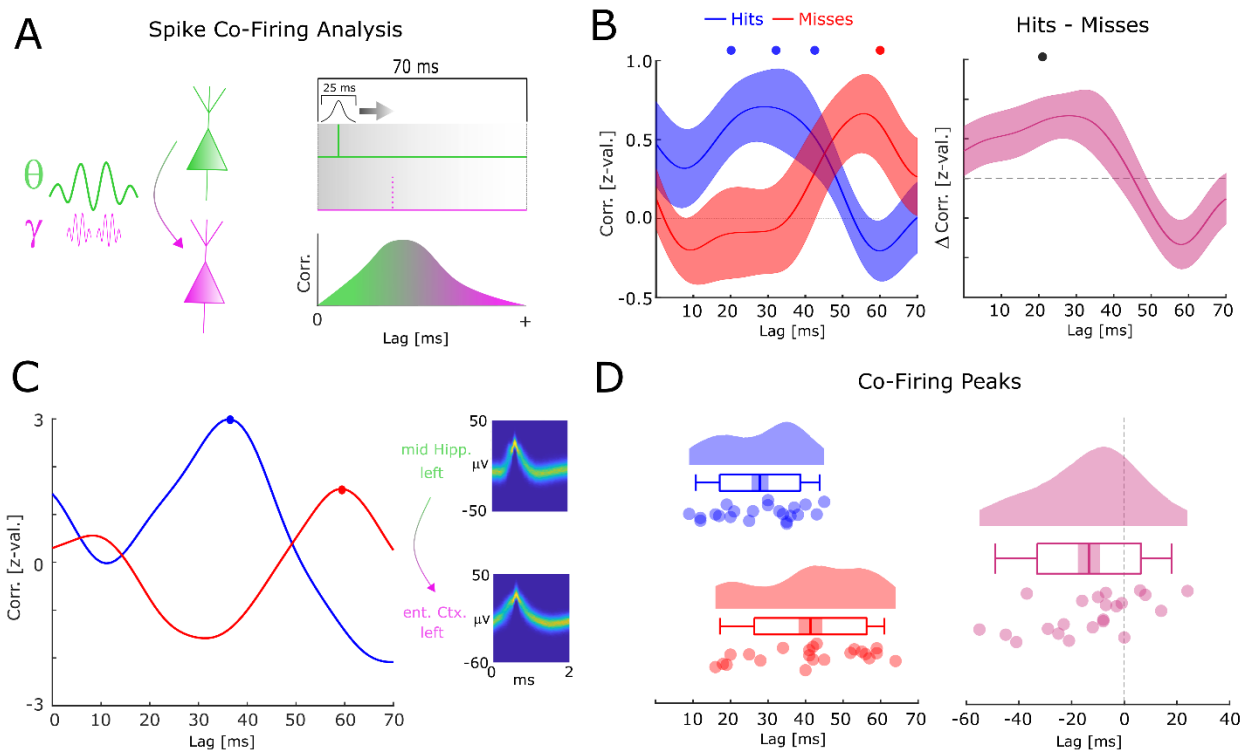

Figure 5. Co-firing analysis results for theta-gamma coupled assemblies. (A) A schematic of the co-firing analysis is shown. Pairs of putative up-stream (green) and putative down-stream (pink) units were selected for the co-firing analysis. Co-firing was measured by cross-correlating spike time series (convolved with a Gaussian envelope). Cross-correlations indicate the latency of firing of a putative down-stream neuron (pink) in response to a putative up-stream neuron (green). (B) Spike cross-correlations for hits and misses are plotted in terms of z-values derived from a trial shuffling procedure. Hits (blue) show increased co-firing between putative up-stream and putative down-stream neurons at around 20-40 ms (p_{corr}<0.05), whereas misses (red) peak at 60 ms (p_{corr}<0.05). Shaded areas indicate standard error of the mean. Differences between co-firing of hits and misses is plotted on the right. Hits show higher co-firing at 20 ms compared to misses (p_{corr}<0.05). (C) Co-firing data is shown for one example pair of units. (D) Results of the co-firing peak detection analysis. The distribution of the peak lag is shown for hits (blue) and misses (red), and for the difference for each pair of neurons (pink). Hits exhibit significantly shorter lags of co-firing compared to misses (p<0.005).

Computational modelling of results in relation to synaptic plasticity

The above results suggest that successful memory formation is supported by a shift of theta and gamma frequencies (Figures 2 and 3), an increase in theta-to-gamma coupling (Figure 4), as well as shorter latencies of co-firing between putative up-stream and down-stream assemblies (Figure 5). Thus, we next examined if this shift in theta/gamma peak-frequency could lead to more efficient neural information transmission and increased synaptic plasticity. To address these questions, we explored the consequences of slower vs. faster rhythms on neural co-firing and synaptic plasticity in a computational model which simulated up-stream theta and down-stream gamma cell assemblies (Figure 6A) as observed in our data. Up-stream neurons were synchronized to a theta rhythm and transmitted their activity to a down-stream assembly which in turn was locally synchronized to a gamma rhythm. Hit trials were simulated by setting the theta frequency to 9 Hz and the gamma frequency to 70 Hz; for miss trials theta was set to 5 Hz and gamma to 60 Hz. In

addition, gamma amplitude to theta phase coupling was set to be higher for hits compared to misses.

Model behavior is shown for a successful (hit) trial and an unsuccessful (miss) trial in Figure 6B. The differences in theta and gamma frequencies are apparent in the raster plots showing a tighter packaging of spikes for the hit trial compared to the miss trial. This difference in frequency and theta-to-gamma coupling had a dramatic effect on synaptic plasticity as modeled by STDP, with hits showing ~250 % increase in synaptic weights, whereas misses barely show a weight increase (Figure 6C).

The observed correlation between the co-firing and synaptic plasticity in our computational model can be unequivocally attributed to the change in the peak frequencies of theta and gamma oscillation. Thus, the present results show that a shift in the peak frequency of theta and gamma oscillations directly affects synaptic plasticity. This suggests that neural synchronization at fast theta and gamma frequencies could be an efficient one-shot learning mechanism underlying episodic memory formation*(9)*.

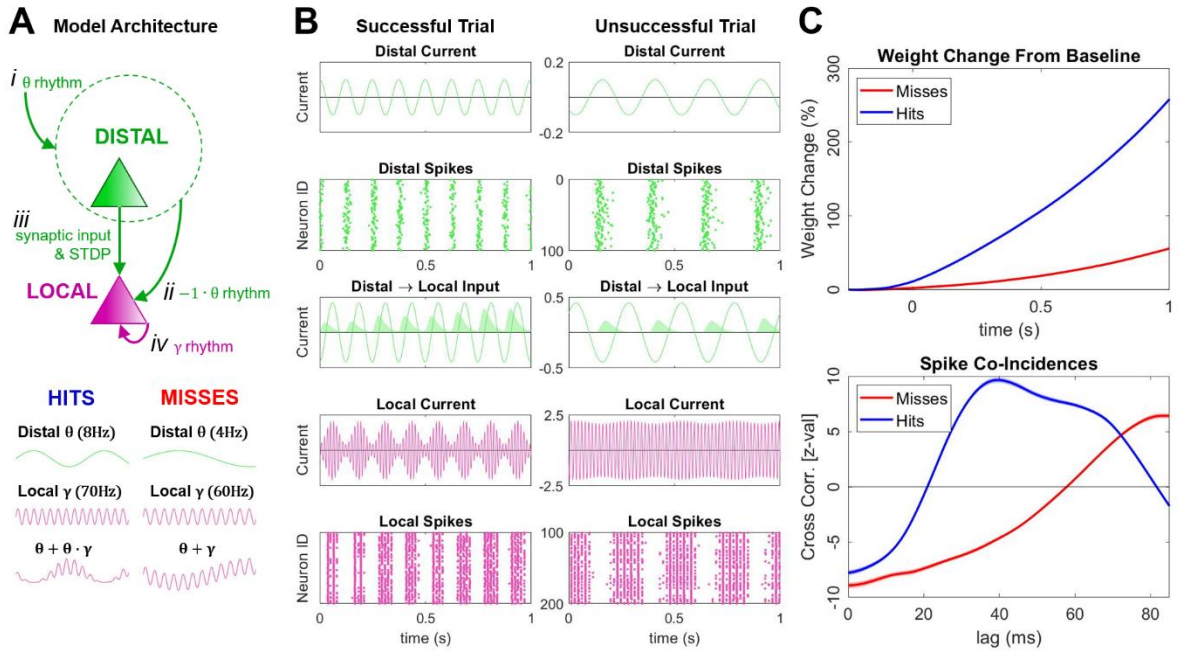

Figure 6. Computational model demonstrating the impact of slow/fast oscillations on spike-timing dependent plasticity (STDP). (A) Model architecture. A set of distal neurons (green) receive a θ-rhythm (i). This θ-rhythm filters through the hippocampus, resulting in a set of local neurons (purple) receiving a phase-reversed θ-rhythm (ii). Distal neurons connect to local neurons (iii), such that weighted distal spikes cause post-synaptic potentials in local neurons and spike-timing-dependent-plasticity (STDP) increases these weights over time. Local neurons also receive a γ-rhythm that is modulated to some degree by the incoming θ-rhythm (iv). For "hits" (blue), distal θ-frequency is 9Hz & γ-frequency is 70Hz, with a high degree of θ:γ cross-frequency coupling. For "misses" (red), distal θ-frequency is 5Hz & γ-frequency is 60Hz, with a low degree of θ:γ cross-frequency coupling. (B) A simulation of a single trial through time for "hits" (left) and "misses" (right). The amplitude of a distal θ-rhythm (top panel) causes spike events in distal neurons (2nd top panel). Distal spike events then induce post-synaptic potentials in local neurons (middle panel; green shaded), which, alongside a phase-reversed θ-rhythm (middle panel; green line), summarizes distal output to local neurons. These operate in conjunction with a locally entrained θ:γ-rhythm (2nd bottom panel) to cause spike events in local neurons (bottom panel). (C) STDP acts to increase the weights of distal to local synapses through time

for the "hits" condition (blue). This is a much slower process for the "misses" condition (red), indicating the positive correlation between oscillatory frequency and learning in human episodic memory. This is corroborated by the spike co-incidences between distal and local spike pairings (bottom panel) where local spikes are more likely to occur shortly after a distal spike for the "hits" condition (blue), thus increasing the likelihood of STDP operating on the active synapse.

Conclusions

More than seven decades ago Donald Hebb proposed the idea that "neurons that fire together, wire together"(*4*). He argued that correlated neural firing plays a crucial role for laying down the neural connections that make up a memory. Although this principle has been well established by animal studies *(2-3,5)*, a direct correlation between co-firing of neurons and memory formation has so far not been demonstrated in the human brain. Consistent with previous evidence*(2-3)* the present study provides critical evidence in showing that co-firing of neurons at short latencies is correlated with the formation of episodic memories in neurons that are synchronized by local gamma and distal theta oscillations. Furthermore, our study demonstrates that co-firing at shorter lags is associated with a coupled upward shift in the peak frequency of gamma and theta oscillations.

References and Notes

1. E. R. Kandel, The molecular biology of memory storage: a dialogue between genes and synapses. *Science* **294**, 1030-1038 (2001).
2. H. Markram, J. Lubke, M. Frotscher, B. Sakmann, Regulation of synaptic efficacy by coincidence of postsynaptic APs and EPSPs. *Science* **275**, 213-215 (1997).
3. G. Bi, M. Poo, Synaptic modification by correlated activity: Hebb's postulate revisited. *Annu Rev Neurosci* **24**, 139-166 (2001).
4. D. O. Hebb, *The organization of behavior; a neuropsychological theory*. A Wiley book in clinical psychology (Wiley, New York,, 1949), pp. xix, 335 p.
5. V. Wespatat, F. Tennigkeit, W. Singer, Phase sensitivity of synaptic modifications in oscillating cells of rat visual cortex. *J Neurosci* **24**, 9067-9075 (2004).
6. P. Fries, Rhythms for Cognition: Communication through Coherence. *Neuron* **88**, 220-235 (2015).
7. G. Buzsaki, Neural syntax: cell assemblies, synapsembles, and readers. *Neuron* **68**, 362-385 (2010).
8. J. M. Hyman, B. P. Wyble, V. Goyal, C. A. Rossi, M. E. Hasselmo, Stimulation in hippocampal region CA1 in behaving rats yields long-term potentiation when delivered to the peak of theta and long-term depression when delivered to the trough. *J Neurosci* **23**, 11725-11731 (2003).
9. P. T. Huerta, J. E. Lisman, Bidirectional synaptic plasticity induced by a single burst during cholinergic theta oscillation in CA1 in vitro. *Neuron* **15**, 1053-1063 (1995).
10. W. Penfield, B. Milner, Memory deficit produced by bilateral lesions in the hippocampal zone. *AMA Arch Neurol Psychiatry* **79**, 475-497 (1958).
11. M. J. Jutras, E. A. Buffalo, Synchronous neural activity and memory formation. *Curr Opin Neurobiol* **20**, 150-155 (2010).
12. J. Fell, N. Axmacher, The role of phase synchronization in memory processes. *Nat Rev Neurosci* **12**, 105-118 (2011).
13. U. Rutishauser, I. B. Ross, A. N. Mamelak, E. M. Schuman, Human memory strength is predicted by theta-frequency phase-locking of single neurons. *Nature* **464**, 903-907 (2010).
14. B. Griffiths *et al.*, Directional coupling of slow and fast hippocampal gamma with neocortical alpha/beta oscillations in human episodic memory. *Proc Natl Acad Sci U S A* **in press**, (2019).
15. J. F. Burke, A. G. Ramayya, M. J. Kahana, Human intracranial high-frequency activity during memory processing: neural oscillations or stochastic volatility? *Curr Opin Neurobiol* **31**, 104-110 (2015).
16. G. Buzsaki, E. W. Schomburg, What does gamma coherence tell us about inter-regional neural communication? *Nat Neurosci* **18**, 484-489 (2015).

17. S. N. Jacob, D. Hahnke, A. Nieder, Structuring of Abstract Working Memory Content by Fronto-parietal Synchrony in Primate Cortex. *Neuron* **99**, 588-597 e585 (2018).
18. S. Liebe, G. M. Hoerzer, N. K. Logothetis, G. Rainer, Theta coupling between V4 and prefrontal cortex predicts visual short-term memory performance. *Nat Neurosci* **15**, 456-462, S451-452 (2012).
19. M. Vinck, M. van Wingerden, T. Womelsdorf, P. Fries, C. M. Pennartz, The pairwise phase consistency: a bias-free measure of rhythmic neuronal synchronization. *Neuroimage* **51**, 112-122 (2010).
20. S. Michelmann, H. Bowman, S. Hanslmayr, The Temporal Signature of Memories: Identification of a General Mechanism for Dynamic Memory Replay in Humans. *PLoS Biol* **14**, e1002528 (2016).
21. A. B. Tort, R. W. Komorowski, J. R. Manns, N. J. Kopell, H. Eichenbaum, Theta-gamma coupling increases during the learning of item-context associations. *Proc Natl Acad Sci U S A* **106**, 20942-20947 (2009).
22. J. Aru *et al.*, Untangling cross-frequency coupling in neuroscience. *Curr Opin Neurobiol* **31**, 51-61 (2015).

Acknowledgments

We like to thank all patients for participating in the experiments. We thank Markus Siegel for useful comments on previous versions of the manuscript. S.H. was supported by grants from the European Research Council (Nr. 647954), and the Economic and Social Research Council (ES/R010072/1). M.tW. and MW were supported by a grant from the European Research Council (StG-715714).